Basic study on estimation method of shear stress in carotid artery using blood flow imaging

血流動態イメージングを用いた頸動脈における Shear stress 推定法に関する基礎検討

Ryo Nagaoka[1], Kazuma Ishikawa[1], Michiya Mozumi[1], Magnus Cinthio[2], and Hideyuki Hasegawa[1]
([1] University of Toyama, Toyama, Japan; [2] Lund University, Lund, Sweden)
長岡　亮[1]，石川　数馬[1]，茂澄倫也[1]，シンチオ　マグナス[2]，長谷川英之[1]
([1] 富山大院，[2] ルンド大学)

1. Introduction

Wall shear stress (WSS), which is a mechanical force acting on the inner surface of the arterial wall. WSS isinduced by blood flow and influences the physiological state of endothelial cells. The endothelial cells generate nitric oxide (NO), having anti-arteriosclerosis effects. When they are stimulated by WSS. Several research groups developed WSS measurement techniques based on a conventional Doppler method[1,2)] and echo particle image velocimetry (PIV) method with microbubbles[3,4)]. However, there is an issue that 2-dimensional (2D) blood flow vector cannot be obtained non-invasively.

Meanwhile, plane wave ultrasonic imaging method[5)] achieves high tempral resoluiton and enables visualization of the blood flow dynamics[6)]. Our group developed blood flow imaging method[7)] visiulizaing echo signals from blood cells themselves using the high temporal ultrasonic imaging and singular value decomposition (SVD) filter[8)]. Additionally, 2D blood flow vectors can be estimated by combining a speckle tracking method with the above-mentioned blood flow imaging method.

In this study, we investigate two WSS estimation techniques based on the measured blood flow vectors. One is to estimate the shear rate from the spatial gradient of the blood flow velocity along a vessel, and the other is to estimate the shear rate from the maximum value of the blood flow velocity. We apply the two techniques to *in vivo* data in the common carotid artery of a 31-year-old healthy male.

2. Materials and Methods

WSS τ is the force field acting along the vessel wall and is expressed as:

$$\tau = \eta\gamma = \eta\frac{\partial v}{\partial r}, \qquad (1)$$

where variables η, v, γ, and r are the fluid viscosity, flow velocity along vessels, shear rate, and distance from the internal surface of the arterial wall, respectively. In this study, the fluid visosisty η is assumed to be 0.003 Pa·s .Two estimation techniques of the shear rate γ was employed as a comparison. The WSS at a posterior wall was estimated using two methods.

2.1 Shear rate estimated from velocity gradient[1-4)]

The Shear rate was obtained by calculating the spatial gradient of the flow velocity profile from a boundary between lumen and artery wall. The flow velocity was estimated using blood speckle visualization and a speckle tracking method. The boundary was defined a position with a velocity estimate of 0 mm/s.

2.2 Shear rate estimated from maximum velocity[9)]

By assuming the flow velocity as laminar flow in the artery, the flow velocity profile along the radial direction is parabolic. Under this assumption, the mean shear rate $\bar{\gamma}$ across an area of the artery is given by the following equation.

$$\bar{\gamma} = \frac{2v_{max}}{R}\left(\frac{n}{n+1}\right), \qquad (1)$$

where variables v_{max}, R, and n are the maximum velocity, radius of the artery, and parameter for the flow velocity profile. Under this assumption, the parameter n = 2.

2.3 Experimental setup

Ultrasonic echo signals were received using 7.5-MHz linear array ultrasonic probe and programable acquisition system. The sampling frequency was set at 62.5 MHz To achieve high frame rate, plane-wave based imaging was employed. RF echo signals from a common carotid artery (CCA) of a 31-year-old healthy male were acquired in a frame rate of 3906 Hz.

3. Results and Discussions

Figure 1 shows an ultrasonic image of the common

* nryo@eng.u-toyama.ac.jp

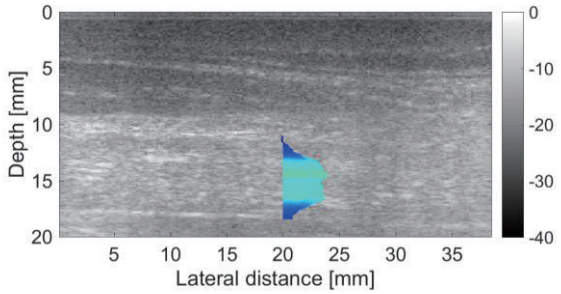

Fig. 1 Blood flow imaging of common carotid artery with 2D velocity vector.

carotid artery with the estimated 2D velocity vectors. **Figure 2** shows the estimated flow velocity profile along the radial direction of the artery corresponding to the 2D velocity shown in **Fig. 1**. Two red dots correspond to the boundary between the lumen and arterial wall, and a black dot shows the position with the maximum velocity. A dotted line corresponds to a linear approximated line calculated by applying the least-square method to the velocity profile. Using the estimated spatial velocity gradient and maximum velocity, the shear rate was calculated by each method to estimate the WSS.

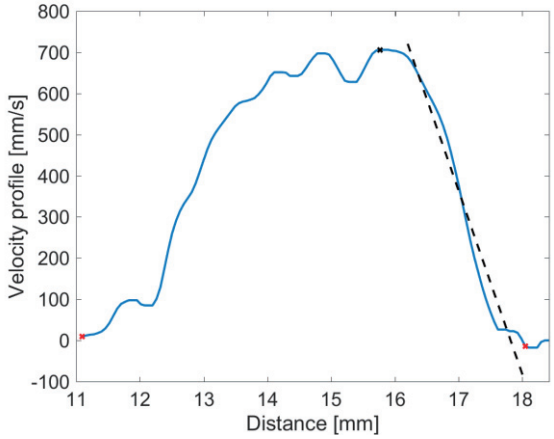

Fig. 2 Flow velocity profile along the radial direction. Two red dots: Boundary between lumen and wall. Black dot: Maximum velocity. Dotted line: Spatial gradient of velocity profile.

Figure 3 shows temporal changes of the estimated WSS. Blue and red dotted line correspond to the WSS estimated from the maximum velocity and spatial velocity gradient, respectively. There is a slight difference on the estimated results. This was because the blood flow was assumed to be laminar flow in the second method. As shown in **Fig. 1**, the velocity profile was not observed as a parabolic profile.

4. Conclusion

In this study, we investigated the two WSS estimation technique from the measured blood flow vector. The WSS estimated from the spatial gradient of blood flow velocity was compared with that from maximum flow velocity. A difference on the estimated results was observed. It was considered that this was because the blood flow was assumed to be laminar flow.

In future work, we will perform simulation experiments using computational fluid dynamics (CFD) to verify the estimation accuracy.

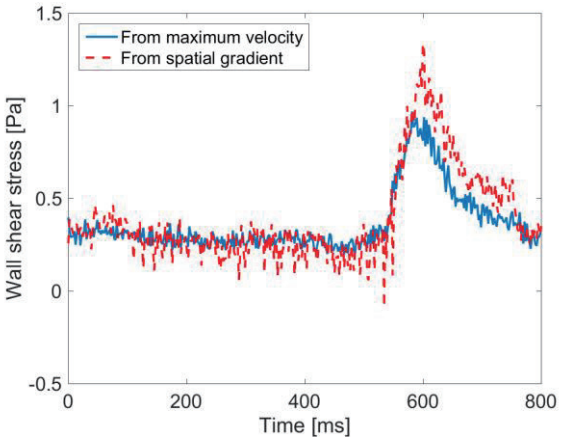

Fig. 3 Temporal changes of WSS. Blue line: Estimation from the maximum velocity. Red dotted line: Estimation from the spatial gradient.

References

1. P. J. Brands, A. P. G. Hoeks, L. Hofstra, and R. S. Reneman: Ultrasound Med. Biol. **22** (1995) 171.
2. N. Nitta and K. Homma: Trans. Jpn. Soc. Med. Biol. Eng. **44** (2006) 190.
3. A. Gurung, P. E. Gates, L. Mazzaro, J. Fulford, F. Zhang, A. L. Barker, J. Hertzberg, K. Aizawa, W. D. Strain, S. Elyas, A. C. Shore and R. Shandas: Ultrasound Med. Biol. **43** (2017) 1618.
4. P. E. Gates, A. Gurung, L. Mazzaro, K. Aizawa, S. Elyas, W. D. Strain, A. C. Shore, and R. Shandas: Ultrasound Med. Biol. **44** (2018) 1392.
5. M. Tanter, J. Bercoff, L. Sandrin, and M. Fink: IEEE Trans. Ultrason. Ferroelectr. Freq. Control **49** (2002) 1363.
6. S. Fadnes, S. Bjærum, H. Torp, and L. Løvstakken: IEEE Trans. Ultrason. Ferroelectr. Freq. Control **62** (2015) 2079.
7. Demené C, Deffieux T, Pernot M, B. F. Osmanski, V. Biran, J. L. Gennisson, L. A. Sieu, A. Bergel, S. Franqui, J. M. Correas, I. Cohen, O. Baud, and M. Tanter, IEEE Trans. Med. Imag. **34** (2015) 2271.
8. M. Mozumi, R. Nagaoka and H. Hasegawa: J. Appl. Phys. **58** (2019) SGGE02.
9. G. Cloutier, Z. Qin, L. G. Durand, B. G. Teh: IEEE Trans Biomed Eng. **43** (1996) 441.